

## Cavity Detuning and Multimode Operation of an Optically Pumped Gas Laser

James J. Healy and T. F. Morse  
*Division of Engineering and Center for Fluid Dynamics,*  
*Brown University, Providence, Rhode Island 02912*  
 (Received 13 April 1972)

In an earlier paper, the problem of the optically pumped gas laser was treated within the formalism of a modified Boltzmann equation and the equation of radiative transfer. The laser cavity was tuned precisely to the center of the atomic lasing frequency and only one cavity mode was excited above threshold. These restrictions are now removed and the effects on the laser population inversion, gain, and power output are presented. In the limit that Doppler broadening dominates collisional broadening, it is found that the power output for the single-mode operation increases as the laser cavity is detuned, until an optimum occurs when the cavity detuning is equal to the collisional linewidth. In the limit that collisional broadening dominates Doppler effects, power output is independent of detuning, until the detuning approaches the collisional linewidth. For multimode operation, it is shown that power output increases approximately linearly with the number of modes in oscillation, provided that the Doppler width is much larger than the collisional width and mode interaction is not occurring. When collisional broadening dominates, no increase in total power output is achieved by allowing more than one mode to go into oscillation. Most of these results are well known, for low levels of lasing intensity, through the semiclassical analysis of Lamb. However, the formulation here provides a more quantitative evaluation of the relative roles of inhomogeneous and homogeneous broadening for all collisional linewidths and high lasing intensities.

### I. INTRODUCTION

Cipolla and Morse<sup>1</sup> have employed a modified Boltzmann equation and the equation of radiative transfer to describe in detail the interaction of line radiation with a gas. These equations are similar to, but more general than, the formulation of Bibermann<sup>2</sup> and Holstein<sup>3</sup> and were applied to the problem of the optically pumped gas laser by Healy and Morse.<sup>4</sup> It was found there that one could obtain a detailed solution for such quantities as the population inversion, gain coefficient, and output power in terms of the optical variables, collision cross sections, and atomic parameters. The analysis was restricted to the situation in which the laser cavity was tuned exactly to the center of the atomic lasing transition, and only one cavity mode was allowed to be excited above threshold. More general formulations involving coupled kinetic and radiation equations exist,<sup>5,6</sup> but their complexity almost precludes their use in seeking analytic solutions to problems where spatial inhomogeneities or nonlinear phenomena appear. In the present paper, the formulation of Ref. 4 is generalized to include cavity detuning and multimode operation. In the following, the formulation of the problem is briefly reviewed, and then the case of a single detuned cavity mode above threshold is considered. The situation in which two modes are excited above threshold is treated in detail, and some general conclusions are drawn for more than two modes in operation. Finally, comparisons are made, where appropri-

ate, with the earlier work of Lamb.<sup>7</sup> It should be noted that although this study is restricted to the optically pumped gas laser, if one regards the excitation rate as a parameter of the problem, the results are then qualitatively applicable to any type of gas laser.

### II. THEORETICAL FORMULATION

Consider a Fabry-Perot cavity formed by two plane mirrors of depth  $2D$  and length  $2L$ , as shown schematically in Fig. 1. The lasing gas is contained between the two mirrors by means of transparent walls, and pumping radiation at approximately the resonance frequency  $\nu_{20}$  is supplied to the laser through these walls. The lasing radiation at frequency  $\nu_{21}$  propagates between the semi-transparent mirrors, and the cavity dimension  $2L$  is such that one or more longitudinal cavity modes lie within the Doppler width of the lasing gas at

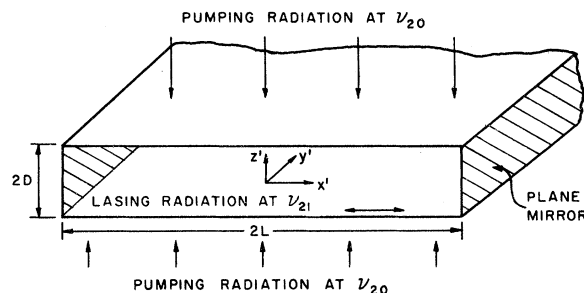


FIG. 1. Geometry of laser.

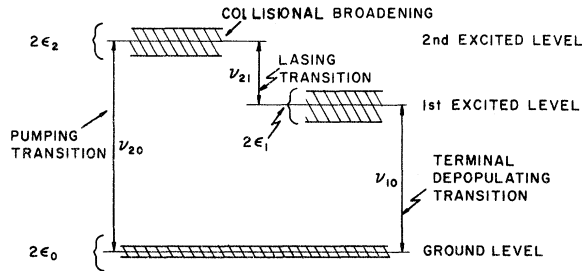


FIG. 2. Description of atomic energy-level model.

$\nu_{21}$ . The oscillation frequencies of the modes which are excited above threshold will be approximately determined by the passive cavity, but frequency-pulling effects cause the actual oscillation to occur at frequencies slightly removed from those of the passive cavity.<sup>7</sup>

In the atomic model adopted here, a ground-state level and two excited-state levels are present, and for simplicity all degeneracies are assumed to be unity. The levels are allowed to have a collisional halfwidth  $\epsilon_0$ ,  $\epsilon_1$ , and  $\epsilon_2$  (see Fig. 2). For purposes of this work, these widths correspond to the homogeneous broadening of the energy levels caused by any process other than Doppler shifting. For the optically pumped laser, efficient utilization of the power source requires that the atomic transition frequency  $\nu_{20}$  corresponds very closely with the frequency of the pumping radiation externally supplied, and in addition, one or more cavity resonance frequencies must be close to the atomic frequency  $\nu_{21}$ . The optically pumped laser is analyzed because the complex collision phenomena associated with other types of lasers are thereby avoided, and one can obtain a self-contained solution for many of the macroscopically observable quantities without making any *ad hoc* assumption regarding the rate of excitation or the atomic velocity distribution function. The best-known example of this type of laser is Cs vapor pumped by a strong He emission line.<sup>8</sup> In addition, the possibility of broad-band pumping of a  $N_2$ - $CO_2$  system by sunlight is currently under investigation.<sup>9</sup>

As discussed in Ref. 4, the governing kinetic equations may be approximated by

$$\begin{aligned} \frac{\eta_2}{\tau_2} \frac{\partial f_0}{\partial z} &\simeq (M_{w_0} - f_0)\sigma_0 + 4\pi(A_{20}f_2 + A_{10}f_1) \\ &\quad - A_{20}Q_{20}f_0, \\ \frac{\eta_1}{\tau_2} \frac{\partial f_1}{\partial z} &\simeq (M_{w_0} - f_1)\sigma_1 + 4\pi(A_{21}f_2 - A_{10}f_1) \\ &\quad + A_{21}Q_{21}(f_2 - f_1), \quad (1) \\ \frac{\eta_2}{\tau_2} \frac{\partial f_2}{\partial z} &\simeq (M_{w_2} - f_2)\sigma_2 - 4\pi(A_{20}f_2 + A_{21}f_2) \end{aligned}$$

$$+ A_{20}Q_{20}f_0 - A_{21}Q_{21}(f_2 - f_1).$$

Here  $f_i(\eta_x, \eta_z)$  is the velocity distribution function for for atoms in energy level  $i$ , with normalization

$$n_i(z) = \int_{-\infty}^{\infty} \int_{-\infty}^{\infty} f_i(z, \eta_x, \eta_z) d\eta_x d\eta_z;$$

$z$  is the dimensionless separation of the transparent plates;  $\tau_2$  is the mean time of flight for an atom to traverse the distance  $D$ ;

$$z \equiv z'/D, \quad -1 \leq z \leq 1; \quad \tau_2 = D/(2RT_w)^{1/2};$$

$\sigma_i$  denotes collision frequencies for processes which tend to destroy the population inversion and result from a relaxation model of the exact collision integral.<sup>4</sup> Finally, the terms  $Q_{mn}$  are source and sink terms for atoms in levels  $m$  and  $n$  due to emitted and absorbed radiation. If the collisional linewidths of the  $mn$  transition are modeled as indicated in Fig. 3, then it can be shown that<sup>4</sup>

$$\begin{aligned} Q_{mn}(f_\nu) &\equiv \int_{-\infty}^{\infty} d\xi_{mn} \int_{4\pi} d\Omega f_\nu \\ &\times \frac{H(W - (\xi_{mn} - \vec{\eta} \cdot \vec{1}))H(W + (\xi_{mn} - \vec{\eta} \cdot \vec{1}))}{2W}, \quad (2) \end{aligned}$$

where

$$W \equiv \frac{(\epsilon_n + \epsilon_m)C}{\nu_{mn}(2RT_w)^{1/2}}$$

is the dimensionless collisional linewidth for the  $m-n$  transition,

$$\xi_{mn} = \frac{\nu - \nu_{mn}}{\nu_{mn}} \frac{C}{(2RT_w)^{1/2}}$$

is the dimensionless frequency difference based on atomic resonance frequency  $\nu_{mn}$ ,  $H(X)$  is the Heaviside unit step function, and  $f_\nu(\vec{1})$  is the photon distribution function for photons propagating in direction  $\vec{1}$ . A more realistic model for the line shape could be used, but the evaluation of the

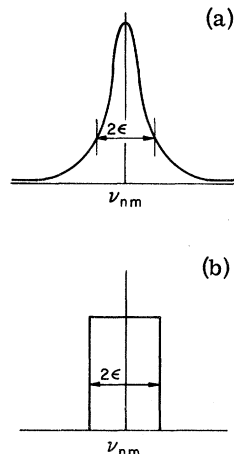


FIG. 3. (a) True collisional line shape. (b) Modeled collisional line shape.

integrals involved would require numerical techniques. The "box" model retains much of the essential physics, and was chosen in the interest of simplicity. The equation of radiative transfer can be replaced by two simpler equations, if there is no overlap between  $\nu_{21}$  and  $\nu_{20}$ , and written as follows<sup>4</sup>:

$$\pm \frac{\partial f_{\nu_{20}}}{\partial z} \approx Dh\nu_{20} B_{20} [\mathcal{J}C_{20}(f_2) - f_{\nu_{20}} \mathcal{J}C_{20}(f_0 - f_2)], \quad (3a)$$

$$\pm \frac{\partial f_{\nu_{21}}}{\partial z} \approx Lh\nu_{21} B_{21} [\mathcal{J}C_{21}(f_2) + f_{\nu_{21}} \mathcal{J}C_{21}(f_2 - f_1)]. \quad (3b)$$

Here  $f_\nu$  refers to photons whose frequency is close to the  $mn$  resonance frequency, and emission profiles are given by<sup>4</sup>

$$\mathcal{J}C_{mn}(f_n) \equiv \int_{-\infty}^{\infty} \frac{C}{\nu_{mn}(2RT_w)^{1/2}} \times \frac{H(W - (\xi_{mn} - \vec{\eta} \cdot \vec{1}))H(W + (\xi_{mn} - \vec{\eta} \cdot \vec{1}))}{2W} f_n(\eta) d\eta. \quad (4)$$

The three kinetic equations and the two radiative equations comprise a set of five coupled integrodifferential equations, as can be seen from the definitions of  $Q_{nm}$  and  $H_{nm}$ . The boundary conditions will be made as simple as possible. It is assumed that atoms leaving a solid surface after a collision are characterized by a Maxwell-Boltzmann distribution and that the pumping radiation at  $z = \pm 1$  is given by

$$f_{\nu_{20}}(z = \pm 1) = \frac{I^0}{\sqrt{\pi}} \delta(1 \mp l_z) e^{-\beta^2 \xi_{20}^2}. \quad (5)$$

That is, the pumping radiation supplied to the laser is highly collimated and is Gaussian in frequency. The Doppler width of the lasing gas divided by the bandwidth of the pumping radiation is defined as  $\beta$  and it is assumed that  $\beta \ll 1$ . The lasing radiation for the  $m$  modes which are excited above threshold is written

$$f_{\nu_{21}} = \sum_m L^m \delta(\xi_m) \delta(1 \pm l_x), \quad (6a)$$

where  $L^m$  is related to the energy in the  $m$ th mode and each  $L^m$  must be self-consistently determined later in the analysis. The oscillation frequency of the  $m$ th mode is  $\xi_{mn}$ , and the frequency separation between two adjacent longitudinal modes is given by

$$\xi_{m+1} - \xi_m \approx \frac{C}{4L} \frac{C}{\nu_{21}(2RT_w)^{1/2}} \equiv \phi_c, \quad (6b)$$

where  $\nu_{21}$  is the frequency of the unbroadened atomic lasing transition and  $L$  is the length of the laser.

### III. ITERATIVE SOLUTION FOR GOVERNING EQUATIONS AND POPULATION INVERSION FOR SINGLE-MODE OPERATION

As discussed in Ref. 4, an iterative solution to the governing equations can be obtained which converges very rapidly, provided

$$h\nu_{20}/kT_w \gg 1$$

and provided that the branching ratio for the upper lasing level is such that

$$A_{20}/\sum_m A_{2m} \ll 1.$$

The temperature of the laser walls  $T_w$  is assumed to be uniform. The restriction on the branching ratio is fulfilled when trapped radiation is not of primary importance, a situation to be avoided in a laser to prevent the formation of a "bottleneck" in the terminal level.<sup>4</sup>

The iteration procedure has been discussed in detail elsewhere<sup>1,4</sup> and involves iterating with Maxwell-Boltzmann values for the velocity distribution functions in the governing equation for the propagation of pumping radiation. Using the boundary conditions (5), the zeroth-order solution for  $f_{\nu_{20}}$  is then quickly found to be

$$f_{\nu_{20}}^{(0)\pm} \approx \frac{I^0}{\sqrt{\pi}} \delta(1 \pm l_z) \exp[-\beta^2 \xi_{20}^2 - S(1 \pm z) e^{-(\xi_{20})^2}]. \quad (7)$$

The  $\pm$  superscripts refer to pumping radiation propagating in the  $+z$  and  $-z$  directions, respectively, and  $S$ , the equilibrium optical depth, is given by

$$S \equiv N\tau_2 C^3 A_{20}/2\sqrt{\pi} \nu_{20}^3.$$

This solution for  $f_{\nu_{20}}^{(0)}$  together with (6) for  $f_{\nu_{21}}$  can now be substituted into the definition (2) to find  $Q_{20}^{(0)}$  and  $Q_{21}^{(0)}$ <sup>4</sup>:

$$Q_{20}^{(0)} = 4\sqrt{\pi} I^0 \cosh(\mu z) e^{-\mu}, \quad (8)$$

where  $\mu \equiv S e^{-\eta^2} z$ , and  $Q_{20}^{(0)}$  is the number of photons in the 2-0 line capable of being absorbed by an atom with velocity  $\eta_x$ . The case is now considered in which only one mode is excited above threshold, and the lasing frequency is not identical to the cavity resonance. Equation (6a) may be rewritten as

$$f_{\nu_{21}}^{(0)} = L^0 \delta(\xi_{21}^1) \delta(1 \pm l_x); \quad (9a)$$

$$\xi_{21} = \xi_{21}^1 \mp \phi, \quad \phi \equiv \frac{C\Delta\nu}{\nu_{21}(2RT_w)^{1/2}}, \quad (9b)$$

and  $\Delta\nu$  is the difference in frequency between the center of the atomic transition and the actual lasing frequency. Using (9a), the following result for  $Q_{21}^{(0)}$  is obtained:

$$Q_{21}^{(0)} = \frac{\pi L^0}{b} [H(b - |\phi| - \eta_x) H(b + |\phi| + \eta_x)]$$

$$+ H(b - |\phi| + \eta_x) H(b + |\phi| - \eta_x), \quad (10)$$

with

$$b \equiv (\epsilon_1 + \epsilon_2) C / \nu_{21} (2RT_w)^{1/2}$$

as the dimensionless collisional linewidth for the lasing transition. The expressions for  $Q_{20}^{(0)}$  and  $Q_{21}^{(0)}$  are now substituted into the kinetic equations (1) and the solution is found as in Ref. 4:

$$f_2^{(1)} - f_1^{(1)} \approx \frac{4\sqrt{\pi} I^0 A_{20} M_{w0} e^{-\mu} [4\pi(A_{10} - A_{21}) + \sigma_1] \cosh \mu z}{[4\pi(A_{20} + A_{21}) + \sigma_2] (4\pi A_{10} + \sigma_1) + [4\pi(A_{10} + A_{20}) + \sigma_1 + \sigma_2] A_{21} Q_{21}^{(0)}}. \quad (11)$$

An expression for the population inversion is found from (11) by integrating over velocity space, and the result is

$$n_2^{(1)} - n_1^{(1)} = \frac{16\sqrt{\pi} e^{-1} I^0 A_{20} N [4\pi(A_{10} - A_{21}) + \sigma_1] \cosh z}{[4\pi(A_{20} + A_{21}) + \sigma_2] (4\pi A_{10} + \sigma_1) S(2 \ln S)^{1/2}} \left( \operatorname{erfc}(b + |\phi|) + \frac{\operatorname{erf}(b + |\phi|) - \operatorname{erf}(b - |\phi|)}{1 + x_0} + \frac{\operatorname{erf}(b - |\phi|)}{1 + 2x_0} \right), \quad |\phi| \leq b \quad (12a)$$

$$n_2^{(1)} - n_1^{(1)} = \frac{16\sqrt{\pi} e^{-1} I^0 A_{20} N [4\pi(A_{10} - A_{21}) + \sigma_1] \cosh z}{[4\pi(A_{20} + A_{21}) + \sigma_2] (4\pi A_{10} + \sigma_1) S(2 \ln S)^{1/2}} \left( \operatorname{erfc}(b + |\phi|) + \operatorname{erf}(|\phi| - b) + \frac{\operatorname{erf}(|\phi| + b) - \operatorname{erf}(|\phi| - b)}{1 + x_0} \right), \quad |\phi| \geq b \quad (12b)$$

where

$$x_0 \equiv \frac{\pi A_{21} L^0 [4\pi(A_{10} + A_{20}) + \sigma_1 + \sigma_2]}{b [4\pi(A_{20} + A_{21}) + \sigma_2] (4\pi A_{10} + \sigma_1)}.$$

The following observations on the population inversions should be noted:

$$\lim_{L^0 \rightarrow 0} (n_2^{(1)} - n_1^{(1)}) = \frac{16\sqrt{\pi} e^{-1} I^0 A_{20} N [4\pi(A_{10} - A_{21}) + \sigma_1] \cosh z}{S(2 \ln S)^{1/2} [4\pi(A_{20} + A_{21}) + \sigma_2] (4\pi A_{10} + \sigma_1)}. \quad (13a)$$

This expression is independent of both detuning and collisional broadening and is identical to the expression one obtains for an optically pumped slab of gas without end mirrors. For zero collisional linewidth,

$$\lim_{b \rightarrow 0, \phi \neq 0} (n_2^{(1)} - n_1^{(1)}) = \frac{16\sqrt{\pi} e^{-1} I^0 A_{20} N [4\pi(A_{10} - A_{21}) + \sigma_1] \cosh z}{S(2 \ln S)^{1/2} [4\pi(A_{20} + A_{21}) + \sigma_2] (4\pi A_{10} + \sigma_1)}. \quad (13b)$$

Thus, regardless of detuning, the lasing frequency is unable to interact effectively with the excited atoms if there is no broadening of the lasing transition.<sup>4</sup>

Finally, the following may be obtained:

$$\lim_{\phi \rightarrow \infty, \phi \gg b, b \neq 0} (n_2^{(1)} - n_1^{(1)}) = \lim_{b \rightarrow 0, \phi \neq 0} (n_2^{(1)} - n_1^{(1)}). \quad (13c)$$

This shows that if the detuning of the cavity is very

much larger than either the Doppler width or the collisional width of the lasing transition, then there is no effective cavity feedback, and the population inversion again approaches that for an optically pumped gas slab of zero collisional width.

#### IV. GAIN, LASING INTENSITY, AND OUTPUT POWER FOR SINGLE-MODE OPERATION

From Eqs. (3b) and (4), the gain of the laser for  $l_x = +1$  may be defined as follows:

$$G^{(1)}(\xi_{21}, z) = Lh\nu_{21} B_{21} \mathcal{C}_{21} (f_2 - f_1) = \frac{4I^0 A_{20} N L C^3 A_{21} [4\pi(A_{10} - A_{21}) + \sigma_1]}{\sqrt{\pi} b \nu_{21}^3 (2RT_w)^{1/2}} \int_0^\infty d\eta_x \cosh \mu z e^{-\mu} e^{-\eta_x^2} \times \int_{-\infty}^\infty \frac{d\eta_x H(b + \xi_{21} - \eta_x) H(b - \xi_{21} + \eta_x) e^{-\eta_x^2}}{[4\pi(A_{20} + A_{21}) + \sigma_2] (4\pi A_{10} + \sigma_1) + A_{21} Q_{21}^{(0)} [4\pi(A_{20} + A_{10}) + \sigma_1 + \sigma_2]} . \quad (14)$$

Using Eqs. (9b) and (10), the following symmetry properties are easily proved for the gain:

$$G(\phi) = G(-\phi), \quad G(\xi_{21}) = G(-\xi_{21}),$$

$$G(l_x = +1; \xi_{21}) = G(l_x = -1; -\xi_{21}),$$

$$G(z) = G(-z). \quad (15)$$

Thus, in evaluating the integrals in (14) only  $l_x = 1$ ,  $0 \leq \xi_{21} \leq \infty$ , and  $0 \leq \phi \leq \infty$  need be considered. All other cases can be found from (15).

The integration over  $\eta_x$  has been treated elsewhere.<sup>1,4</sup> The integral over  $\eta_x$  is complicated by the fact that it can take on a large number of analytical forms, depending on the relative magnitude of  $b$ ,  $\phi$ , and  $\xi_{21}$ . The results will be presented only for the cases of greatest physical interest.

A detailed example of the evaluation of the integral in one particular case is given in the Appendix.

A normalized gain is defined as follows:

$$\bar{G} \equiv \frac{G^{(1)}(\xi_{21}; L^0; b; \phi)}{G^{(1)}(0; 0; b; \phi)} . \quad (16)$$

After a large amount of tedious but elementary manipulation similar to that in the Appendix, the following results are obtained:

$$\bar{G} = \left( \frac{\text{erf}(b + \xi_{21}) + \text{erf}(b - \xi_{21}) - 2 \text{erf}(b - |\phi|)}{2 \text{erfb}(1 + x_0)} + \frac{\text{erf}(b - |\phi|)}{\text{erfb}(1 + 2x_0)} \right), \quad 0 \leq |\xi_{21}| \leq |\phi| \quad (17a)$$

$$\bar{G} = \left( \frac{\text{erf}(b - \xi_{21}) + \text{erf}(b - |\phi|)}{2 \text{erfb}(1 + 2x_0)} + \frac{\text{erf}(b + |\phi|) - \text{erf}(b - |\phi|)}{2 \text{erfb}(1 + x_0)} + \frac{\text{erf}(b + \xi_{21}) - \text{erf}(b + |\phi|)}{2 \text{erfb}} \right), \quad |\phi| \leq |\xi_{21}| \leq 2b - |\phi| \quad (17b)$$

$$\bar{G} = \left( \frac{\text{erf}(b + \phi) + \text{erf}(b - \xi_{21})}{2 \text{erfb}(1 + x_0)} + \frac{\text{erf}(b + \xi_{21}) - \text{erf}(b + \phi)}{2 \text{erfb}} \right), \quad 2b - |\phi| \leq \xi_{21} \leq 2b + |\phi| \quad (17c)$$

$$\bar{G} = \left( \frac{\text{erf}(b + \xi_{21}) + \text{erf}(b - \xi_{21})}{2 \text{erfb}} \right), \quad 2b + |\phi| \leq \xi_{21} \leq \infty . \quad (17d)$$

Equations (17a)–(17d) all apply to the case  $|\phi| \leq b$ . Similar sets of formulas are found for the cases  $b \leq |\phi| \leq 2b$  and  $2b \leq |\phi| \leq \infty$ . The expressions for the latter two cases are given in the Appendix. The physical content of these expressions is shown in Figs. 4–8. As  $L^0 \rightarrow 0$  (no lasing action), the gain always becomes independent of detuning. For a given lasing intensity and collisional linewidth much less than the Doppler width ( $b \ll 1$ ), the gain has a “hole” which is centered on the actual lasing frequency  $|\xi_{21}| = \phi$ . Thus, as  $\phi$  increases from zero, the hole moves out from the center of the gain curve ( $\xi_{21} = 0$ ). Eventually, for  $\phi \gg 1$  the hole is far out in the tail of the gain curve, and lasing action will cease. For collisional width much larger than the Doppler width ( $b \gg 1$ ), the hole disappears, and for a given lasing intensity, the value of  $\phi$  is immaterial, provided  $\phi < b$  (see Fig. 8). The physical reason for the behavior is clear when one recalls that the “hole” is caused by the fact that only atoms with a limited velocity range can interact with the lasing radiation when  $b \ll 1$ , while all atoms can interact when  $b \gg 1$ .<sup>4</sup> Thus when  $b \ll 1$ ,

detuning the cavity causes the frequency difference between the cavity resonance and the atomic resonance to become larger, the region of velocity space with which atoms can interact is shifted, and the hole moves toward the wings of the gain curve. For  $b \gg 1$ , all atoms can interact with the lasing radiation, unless  $\phi$  becomes so large that the lasing frequency corresponds to the tail of the gain. For  $\phi < b$ , however, the gain will be insensitive to  $\phi$ .

Consider now the effect of detuning on power output for single-mode operation. First, the self-consistent value of the lasing intensity  $L^0$  will be investigated by requiring that steady-state gain equal steady-state loss, at the lasing frequency given by  $\xi_{21} = \phi$ .<sup>10</sup> Thus

$$G(\xi_{21} = \phi) \equiv \frac{1}{2} f, \quad (18)$$

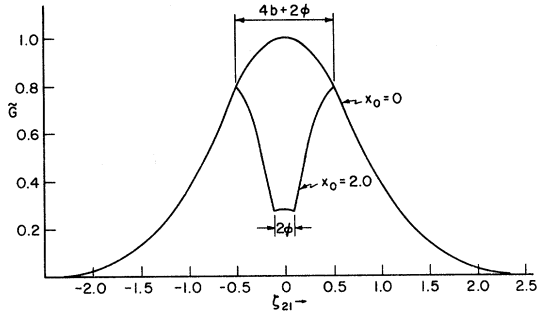
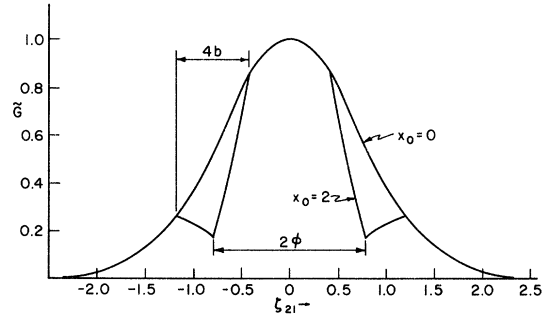
where  $e^{-f}$  is the fraction of photons which survive one trip along the laser axis in one direction, when no amplifying medium is present. From (14), (17a), and (18) the following results may be obtained:

$$\frac{f}{2} = \frac{2\pi e^{-1} I^0 A_{21} [4\pi(A_{10} - A_{21}) + \sigma_1]}{b(2 \ln S)^{1/2} [4\pi(A_{20} + A_{21}) + \sigma_2] (4\pi A_{10} + \sigma_1)} \frac{L}{D} \left( \frac{\nu_{20}}{\nu_{21}} \right)^3 \left( \frac{\text{erf}(b + |\phi|) - \text{erf}(b - |\phi|)}{1 + x_0} + \frac{2 \text{erf}(b - \phi)}{1 + 2x_0} \right), \quad |\phi| \leq b \quad (19a)$$

$$\frac{f}{2} = \frac{2\pi e^{-1} I^0 A_{21} [4\pi(A_{10} - A_{21}) + \sigma_1]}{b(2 \ln S)^{1/2} [4\pi(A_{20} + A_{21}) + \sigma_2] (4\pi A_{10} + \sigma_1)} \frac{L}{D} \left( \frac{\nu_{20}}{\nu_{21}} \right)^3 \frac{\text{erf}(b + |\phi|) + \text{erf}(b - |\phi|)}{1 + x_0}, \quad |\phi| \geq b . \quad (19b)$$

From either of these equations, the threshold pumping intensity  $I^*$  may be obtained by setting  $x_0 = 0$  and solving for  $I^0$ . For a specific value of  $\phi$  the pumping intensity at which lasing action can begin is given by  $I^*$ . Thus (for  $z = 0$ ),



FIG. 5. Normalized gain for  $b=0.2$ ;  $\phi=0.1$ .FIG. 6. Normalized gain for  $b=0.2$ ;  $\phi=0.8$ .

pulling effects, will be as shown in Fig. 10. As before,  $\zeta_{21}=0$  defines the center of the atomic resonance line. In general, the two lasing modes will be displaced from the center at  $\zeta_{21}=\phi_0$  and  $\zeta_{21}=-\phi_1$  as shown, with  $\phi_C=\phi_0+\phi_1$ . The separation between the two lasing modes is given by Eq. (6b). From Eq. (6a) for the bimodal operation,  $f_{\nu_{21}}$  becomes

$$f_{\nu_{21}} = [L^0 \delta(\zeta_{21}^0) + L^1 \delta(\zeta_{21}^1)] \delta(1 \pm l_x) \\ = [L^0 \delta(\zeta_{21} - \phi_0) + L^1 \delta(\zeta_{21} + \phi_1)] \delta(1 \pm l_x); \quad (24)$$

substituting (24) into (2) yields

$$Q_{21}^{(0)} = \frac{\pi L^0}{b} [H(b + |\phi_0| - \eta_x) H(b - |\phi_0| + \eta_x)$$

$$+ H(b + |\phi_0| + \eta_x) H(b - |\phi_0| - \eta_x)] \\ + \frac{\pi L^1}{b} [H(b - |\phi_1| - \eta_x) H(b + |\phi_1| + \eta_x) \\ + H(b - |\phi_1| + \eta_x) H(b + |\phi_1| - \eta_x)], \quad (25)$$

where  $Q_{21}^{(0)}$  is given by Eq. (8), and the solution for  $(f_2^{(1)} - f_1^{(1)})$  is given as before by Eq. (11), with (25) replacing the earlier Eq. (10). When the distribution functions are integrated over velocity space, there are three independent parameters to be considered,  $\phi_0$ ,  $\phi_C$ , and  $b$ . The analytic expressions for  $(n_2^{(1)} - n_1^{(1)})$  for all relative magnitudes are too lengthy to be given here, and only some of the most significant cases are considered:

$$n_2^{(1)} - n_1^{(1)} = \frac{16\sqrt{\pi}e^{-1}I^0A_{20}N[4\pi(A_{10}+A_{21})+\sigma_1]\cosh(z)}{[4\pi(A_{20}+A_{21})+\sigma_2](4\pi A_{10}+\sigma_1)S(2\ln S)^{1/2}} I, \quad (26)$$

where  $I$  is given by

$$I = \operatorname{erfc}(b + |\phi_0|) + \frac{\operatorname{erf}(b + |\phi_0|) - \operatorname{erf}(b + \phi_1)}{1 + x_0} + \frac{\operatorname{erf}(b + |\phi_1|) - \operatorname{erf}(b - |\phi_1|)}{1 + x_0 + x_1} \\ + \frac{\operatorname{erf}(b - |\phi_1|) - \operatorname{erf}(b - |\phi_0|)}{1 + x_0 + 2x_1} + \frac{\operatorname{erf}(b - |\phi_0|)}{1 + 2x_0 + 2x_1}, \quad 0 \leq \phi_C \leq b, \quad 0 \leq |\phi_0| \leq b \quad (26a)$$

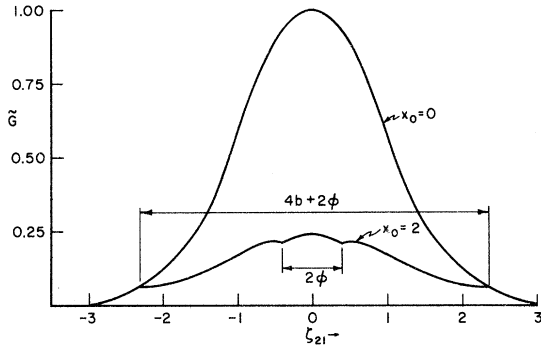
$$I = \operatorname{erfc}(b + |\phi_0|) + \frac{\operatorname{erf}(b + |\phi_0|) - \operatorname{erf}(b + |\phi_1|)}{1 + x_0} + \frac{\operatorname{erf}(b + |\phi_1|) - \operatorname{erf}(b - |\phi_1|)}{1 + x_0 + x_1} \\ + \frac{\operatorname{erf}(b - |\phi_1|) + \operatorname{erf}(b - |\phi_0|)}{1 + x_0 + 2x_1} - \frac{\operatorname{erf}(b - |\phi_0|)}{1 + x_1}, \quad b \leq \phi_C \leq 2b, \quad b \leq |\phi_0| \leq 2b \quad (26b)$$

$$I = \frac{\operatorname{erf}(b - |\phi_1|)}{1 + 2x_1} + \frac{\operatorname{erf}(b + |\phi_1|) - \operatorname{erf}(b - |\phi_1|)}{1 + x_1} + \operatorname{erf}(9b - |\phi_1|) - \operatorname{erf}(b + |\phi_1|) \\ + \frac{\operatorname{erf}(11b - |\phi_1|) - \operatorname{erf}(9b - |\phi_1|)}{1 + x_0} + \operatorname{erfc}(11b - |\phi_1|), \quad \phi_C = 10b, \quad \phi_0 \leq \phi_C, \quad 0 \leq \phi_1 \leq b \quad (26c)$$

where

$$x_1 \equiv \frac{\pi A_{21} L^1 [4\pi(A_{10} + A_{20}) + \sigma_1 + \sigma_2]}{b [4\pi(A_{20} + A_{21}) + \sigma_2] (4\pi A_{10} + \sigma_1)}$$

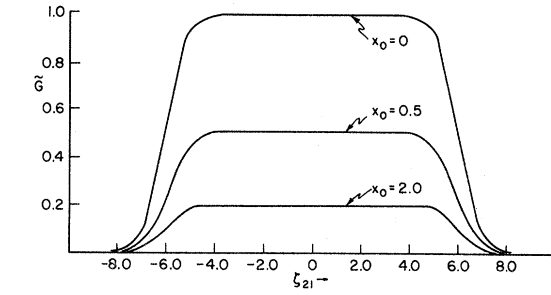
and  $x_0$  has been defined earlier. In all cases, the expressions for  $n_2 - n_1$  reduce to Eq. (13a) as  $L^0$  and  $L^1$  both go to zero. Similar expressions for other values of  $\phi_0$ ,  $\phi_1$ , and  $b$  can easily be

FIG. 7. Normalized gain for  $b=1.0$ ;  $\phi=0.4$ .

found by constructing diagrams as in the Appendix.

From Eqs. (14) and (25), the gain for the bimodal operation can be determined. Again results are given only for the more significant cases:

$$G^{(1)}(\xi_{21}; L^0; L^1; \phi_0; \phi_1; b) = \frac{A_{21} L C^3}{4b\nu_{21}^3 (2RT_w)^{1/2}} \iint (f_2 - f_1) H(b - \xi_{21} + \eta_x) \times H(b + \xi_{21} - \eta_x) d\eta_x d\eta_x, \quad (27)$$

FIG. 8. Normalized gain for  $b=6.0$ ;  $0 \leq |\phi| \leq 4$ .

and, as before, a normalized gain coefficient is defined

$$\tilde{G} \equiv \frac{G^{(1)}(\xi_{21}; L^0; L^1; \phi_0; \phi_1; b)}{G^{(1)}(0; 0; 0; \phi_0; \phi_1; b)}. \quad (28)$$

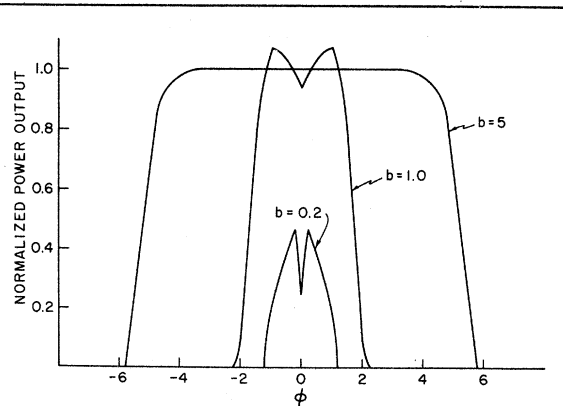
First consider the situation where the collisional linewidth is larger than the frequency separation of cavity resonances ( $b \geq \phi_c$ ). As an example of this situation we choose  $\phi_1 = 0$ ;  $\phi_0 = \phi_c$ ;  $\phi_c < b$ . Then

$$\begin{aligned} \tilde{G} &= \frac{\operatorname{erf}(b) + \operatorname{erf}(b - \xi_{21}) - 2\operatorname{erf}(b - \phi_c)}{2\operatorname{erfb}(1 + x_0 + 2x_1)} + \frac{2\operatorname{erf}(b - \phi_c)}{2\operatorname{erfb}(1 + 2x_0 + 2x_1)} + \frac{\operatorname{erf}(b + \xi_{21}) - \operatorname{erfb}}{2\operatorname{erfb}(1 + x_0)}, \quad 0 \leq \xi_{21} \leq \phi_c \\ \tilde{G} &= \frac{\operatorname{erf}(b - \phi_c) + \operatorname{erf}(b - \xi_{21})}{2\operatorname{erfb}(1 + 2x_0 + 2x_1)} + \frac{\operatorname{erfb} - \operatorname{erf}(b - \phi_c)}{2\operatorname{erfb}(1 + x_0 + 2x_1)} + \frac{\operatorname{erf}(b + \phi_c) - \operatorname{erfb}}{2\operatorname{erfb}(1 + x_0)} + \frac{\operatorname{erf}(b + \xi_{21}) - \operatorname{erf}(b + \phi_c)}{2\operatorname{erfb}}, \quad \phi_c \leq \xi_{21} \leq 2b - \phi_c \\ \tilde{G} &= \frac{\operatorname{erfb} + \operatorname{erf}(b - \xi_{21})}{2\operatorname{erfb}(1 + x_0 + 2x_1)} + \frac{\operatorname{erf}(b + \phi_c) - \operatorname{erfb}}{2\operatorname{erfb}(1 + x_0)} + \frac{\operatorname{erf}(b + \xi_{21}) - \operatorname{erf}(b + \phi_c)}{2\operatorname{erfb}}, \quad 2b - \phi_c \leq \xi_{21} \leq 2b \\ \tilde{G} &= \frac{\operatorname{erf}(b + \phi_c) + \operatorname{erf}(b - \xi_{21})}{2\operatorname{erfb}(1 + x_0)} + \frac{\operatorname{erf}(b + \xi_{21}) - \operatorname{erf}(b + \phi_c)}{2\operatorname{erfb}}, \quad 2b \leq \xi_{21} \leq 2b + \phi_c \\ \tilde{G} &= \frac{\operatorname{erf}(b + \xi_{21}) + \operatorname{erf}(b - \xi_{21})}{2\operatorname{erfb}}, \quad 2b + \phi_c \leq \xi_{21} \leq \infty. \end{aligned} \quad (29)$$

Equations (29) are plotted in Fig. 11 for  $b \gg 1$ . Since all atoms are capable of interaction with the lasing radiation, there are no distinct holes, and the two lasing frequencies are competing for the same excited atoms. In Fig. 12, Eqs. (29) are plotted for  $b = 0.4$ , and since not all atoms are now capable of interaction with the lasing radiation, hole burning is evident. However, the holes overlap since  $\phi_c < 4b$ , and the two lasing frequencies are still in competition for the same atoms.

Consider now the situation in which  $\phi_c > 4b$ , and as an example let  $\phi_1 = 0$ ,  $\phi_0 = \phi_c$ . For this case the following may be shown:

$$\tilde{G} = \frac{\operatorname{erfb} + \operatorname{erf}(b - \xi_{21})}{2\operatorname{erfb}(1 + 2x_1)} + \frac{\operatorname{erf}(b + \xi_{21}) - \operatorname{erfb}}{2\operatorname{erfb}},$$

FIG. 9. Normalized power output vs detuning for fixed  $I^0$ .  $(I^0/I^*)_{\phi=0}$ ,  $b=5=10$ .

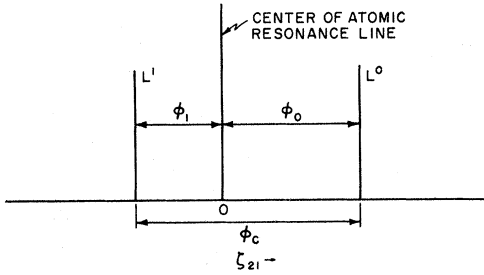


FIG. 10. Location of lasing frequencies for bimodal operation.

$$0 \leq \zeta_{21} \leq 2b$$

$$\tilde{G} = \frac{\text{erf}(b + \zeta_{21}) + \text{erf}(b - \zeta_{21})}{2 \text{erf}b}, \quad 2b \leq \zeta_{21} \leq \phi_c - 2b$$

$$\tilde{G} = \frac{\text{erf}(\phi_c - b) + \text{erf}(b - \zeta_{21})}{2 \text{erf}b} + \frac{\text{erf}(b + \zeta_{21}) - \text{erf}(\phi_c - b)}{2 \text{erf}b(1 + x_0)}, \quad \phi_c - 2b \leq \zeta_{21} \leq \phi_c$$

$$\tilde{G} = \frac{\text{erf}(\phi_c + b) + \text{erf}(b - \zeta_{21})}{2 \text{erf}b(1 + x_0)} + \frac{\text{erf}(b + \zeta_{21}) - \text{erf}(\phi_c + b)}{2 \text{erf}b}, \quad \phi_c \leq \zeta_{21} \leq \phi_c + 2b$$

$$\tilde{G} = \frac{\text{erf}(b + \zeta_{21}) + \text{erf}(b - \zeta_{21})}{2 \text{erf}b}, \quad 2b + \phi_c \leq \zeta_{21} \leq \infty. \quad (30)$$

Equations (30) are plotted on Fig. 13 for  $b \ll 1$ . The holes due to the two lasing lines are now distinct, since each lasing frequency is interacting with a different group of atoms. For  $b \gg 1$ , Eq. (30) becomes identical to Eq. (17) for  $\phi = 0$ . This is because for  $\phi_c \geq b$  and  $b \gg 1$ , the lasing line at  $\zeta_{21} = \phi_c$  is far out in the wings of the gain curve, where the gain is very close to zero even with no lasing. Thus for practical purposes, bimodal operation is not possible for  $\phi_c > b$  with  $b \gg 1$ .

#### VI. POWER OUTPUT FOR BIMODAL OPERATION

The self-consistent lasing intensity is found as before by equating the saturated gain at each lasing

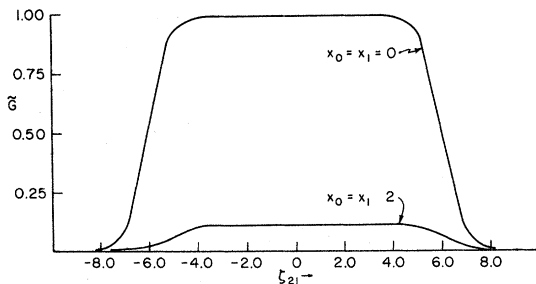


FIG. 11. Bimodal normalized gain;  $b=6.0$ ;  $\phi_1=0$ ;  $\phi_c=1.0$ ;  $x_0=x_1=2$ .

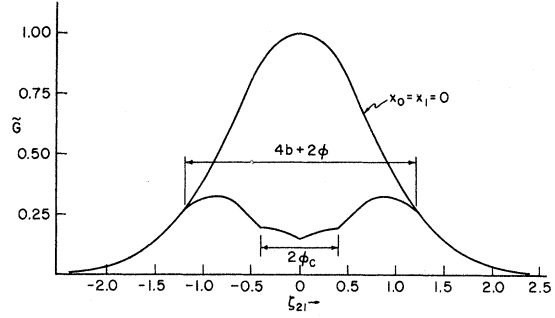


FIG. 12. Bimodal normalized gain;  $b=0.4$ ;  $\phi_1=0$ ;  $\phi_c=0.4$ ;  $x_0=x_1=2$ .

frequency to the cavity losses at that frequency. In situations in which  $\phi_c \geq 4b$ , there is no interaction between the lasing lines, and the intensity of each line is independent of all the others. From Eqs. (30), for example,

$$\frac{f}{2} = \frac{4\pi e^{-1} I^0 A_{21} [4\pi(A_{10} - A_{21}) + \sigma_1]}{b(2 \ln S)^{1/2} [4\pi(A_{20} + A_{21}) + \sigma_2] (4\pi A_{10} + \sigma_1)} \times \frac{L}{D} \left( \frac{\nu_{20}}{\nu_{21}} \right)^3 \frac{\text{erf}b}{1 + 2x_1} \quad (31a)$$

with one line at  $\zeta_{21} = 0$ , and

$$\frac{f}{2} = \frac{2\pi e^{-1} I^0 A_{21} [4\pi(A_{10} - A_{21}) + \sigma_1]}{b(2 \ln S)^{1/2} [4\pi(A_{20} + A_{21}) + \sigma_2] (4\pi A_{10} + \sigma_1)} \times \frac{L}{D} \left( \frac{\nu_{20}}{\nu_{21}} \right)^3 \frac{\text{erf}(\phi_c + b) - \text{erf}(\phi_c - b)}{1 + x_0} \quad (31b)$$

with the other line at  $\zeta_{21} = \phi_c$ . The solutions for  $L^0$  and  $L^1$  are then identical to Eqs. (21) where the appropriate value of  $m$  is fixed by the location of the lasing lines. However, if  $4b \leq \phi_c \ll 1$ , then  $L^0$  and  $2L^1$  are essentially equal, and the total energy stored in the lasing modes is almost triple the amount stored for single-mode operation at  $\zeta_{21} = 0$ . Thus the output power will also be approximately tripled in this case. Figure 14 illustrates the sit-

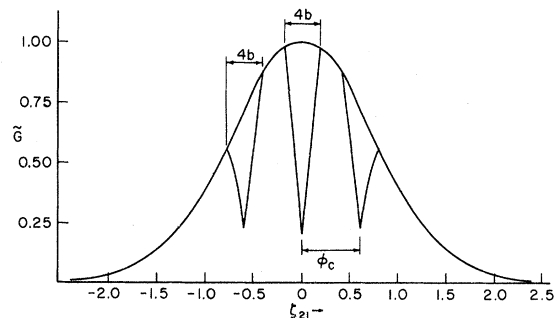


FIG. 13. Bimodal normalized gain;  $b=0.1$ ;  $\phi_1=0$ ;  $\phi_c=0.6$ ;  $x_0=x_1=2$ .

uation where  $b \ll 1$  and two modes are detuned so that they are as close together as possible without being in competition. This situation would yield the maximum power output for bimodal separation (with  $b \ll 1$ ) and the total power is almost double that for a single detuned mode with the same value of  $b$ .  $\phi_c \geq 8b$  is a necessary but not sufficient con-

dition for nonoverlapping holes.

The situation when  $\phi_c < 8b$  is more complex since now there is always some degree of competition between the lasing modes for the same excited atoms, or in terms of hole burning, the holes partially overlap. Using (29) as an example, we find ( $\phi_c \leq b$ ):

$$\frac{f}{2} = \frac{2\pi e^{-1} I^0 A_{21} [4\pi(A_{10} - A_{21}) + \sigma_1]}{b(2\ln S)^{1/2} [4\pi(A_{20} + A_{21}) + \sigma_2] (4\pi A_{10} + \sigma_1)} \frac{L}{D} \left( \frac{\nu_{20}}{\nu_{21}} \right)^3 \left( \frac{2 \operatorname{erf} b - 2 \operatorname{erf}(b - \phi_c)}{1 + x_0 + 2x_1} + \frac{2 \operatorname{erf}(b - \phi_c)}{1 + 2x_0 + 2x_1} \right) \quad (32a)$$

at  $\zeta_{21} = 0$ , and

$$\frac{f}{2} = \frac{2\pi e^{-1} I^0 A_{21} [4\pi(A_{10} - A_{21}) + \sigma_1]}{b(2\ln S)^{1/2} [4\pi(A_{20} + A_{21}) + \sigma_2] (4\pi A_{10} + \sigma_1)} \frac{L}{D} \left( \frac{\nu_{20}}{\nu_{21}} \right)^3 \left( \frac{2 \operatorname{erf}(b - \phi_c)}{1 + 2x_0 + 2x_1} + \frac{\operatorname{erf} b - \operatorname{erf}(b - \phi_c)}{1 + x_0 + 2x_1} + \frac{\operatorname{erf}(b + \phi_c) - \operatorname{erf} b}{1 + x_0} \right) \quad (32b)$$

at  $\zeta_{21} = \phi_c$ . The solution of these simultaneous equation leads, in general, to a quadratic for  $x_0$  or  $x_1$ . Defining  $m = I^0/I^*$ , where  $I^*$  is given by (20), Eqs. (32) may be written

$$\frac{2 \operatorname{erf} b - 2 \operatorname{erf}(b - \phi_c)}{1 + x_0 + 2x_1} + \frac{2 \operatorname{erf}(b - \phi_c)}{1 + 2x_0 + 2x_1} = \frac{\operatorname{erf}(b + \phi_c) + \operatorname{erf}(b - \phi_c)}{m}, \quad \zeta_{21} = 0 \quad (33a)$$

$$\frac{\operatorname{erf} b - \operatorname{erf}(b - \phi_c)}{1 + x_0 + 2x_1} + \frac{2 \operatorname{erf}(b - \phi_c)}{1 + 2x_0 + 2x_1} + \frac{\operatorname{erf}(b + \phi_c) - \operatorname{erf} b}{1 + x_0} = \frac{\operatorname{erf}(b + \phi_c) + \operatorname{erf}(b - \phi_c)}{m}, \quad \zeta_{21} = \phi_c. \quad (33b)$$

For  $\phi_c \ll b$ , Eqs. (33) reduce to

$$x_0 + x_1 \simeq \frac{1}{2}(m - 1). \quad (34)$$

Taking the same limit as in Eq. (21a) one finds, for single-mode operation, that

$$x_0 \simeq \frac{1}{2}(m - 1).$$

Thus when  $\phi_c \ll b$ , the total power output from two oscillating modes is equal to the power from a single mode. This is physically reasonable, since in this limit there is strong competition between the two modes for all of the available excited atoms, and practically no further excited atoms are brought into play if the second mode goes into oscillation.

For  $\phi_c = b$ , Eqs. (33) reduce to

$$\begin{aligned} \frac{2 \operatorname{erf} b}{1 + x_0 + 2x_1} &= \frac{\operatorname{erf} 2b}{m}, & \zeta_{21} &= 0 \\ \frac{\operatorname{erf} b}{1 + x_0 + 2x_1} + \frac{\operatorname{erf} 2b - \operatorname{erf} b}{1 + x_0} &= \frac{\operatorname{erf} 2b}{m}, & \zeta_{21} &= \phi_c. \end{aligned} \quad (35)$$

Solving for  $x_0$  and  $x_1$ , the following results may be obtained:

$$x_1 = m(2 \operatorname{erf} b - \operatorname{erf} 2b) / \operatorname{erf} 2b, \quad (36a)$$

$$x_0 = 2m[\operatorname{erf} 2b - \operatorname{erf} b] / \operatorname{erf} 2b - 1. \quad (36b)$$

For  $b \gg 1$ , these become

$$x_1 \simeq m, \quad x_0 = -1 \quad (\phi_c = b).$$

Thus for  $\phi_c = b$ , bimodal operation is impossible when  $b \gg 1$ . For  $b \ll 1$ , Eqs. (36) become

$$x_1 \simeq m, \quad x_0 \simeq m - 1 \quad (\phi_c = b).$$

Thus the detuned mode will tend to extinguish the mode at the line center when  $b \ll 1$  and  $\phi_c \rightarrow b$ .

For more than two modes in oscillation the following conclusions can now be drawn: When  $\phi_c \geq 8b$ ,  $b \ll 1$ , each mode may interact with a separate group of excited atoms, and the power in each mode is then equal to the power which would be available if that mode alone were in oscillation. When  $\phi_c < 8b$ , there is always some degree of interaction between the oscillating modes, and for  $n$  modes the total power is less than that for  $n$  non-interacting modes. Furthermore, when  $\phi_c \leq 8b$  there are situations in which the equations corresponding to (32) indicate that multimode operation

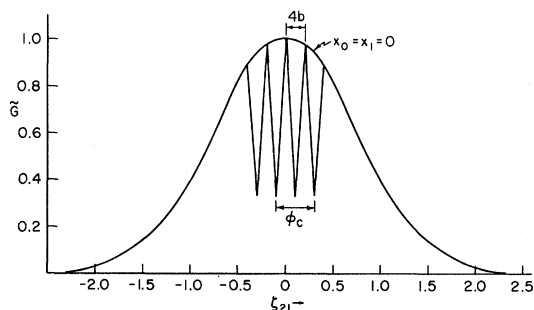


FIG. 14. Normalized gain;  $b=0.05$ ;  $\phi_1=2b$ ;  $\phi_0=6b$ ;  $x_0=1.7$ ;  $x_1=2.0$ .

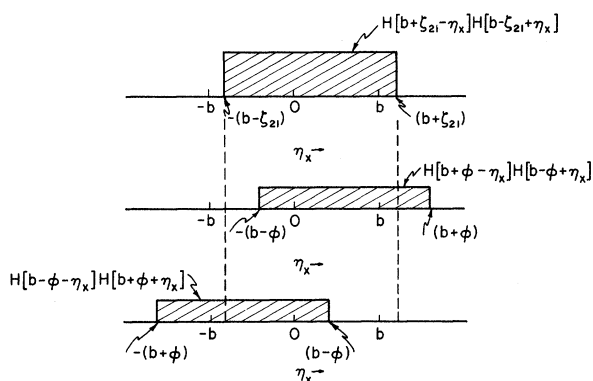


FIG. 15. Behavior of Heaviside functions for  $\zeta_{21} \leq \phi \leq b$ .

is impossible due to mode competition effects. An exhaustive study for any given combination of  $b$ ,  $\phi_0$ , and  $\phi_c$  would require the evaluation of the integrals for the gain. The gain would subsequently be equated at each lasing frequency to the cavity losses. For  $n$  modes this generates, in general, an  $n$ th-order algebraic equation whose solution will indicate under which circumstances two or more modes can simultaneously oscillate. The present work has attempted to illustrate some of the more significant cases.

#### VII. CONCLUSIONS AND COMPARISON WITH WORK OF LAMB

It is of interest to compare the results of the present study with an earlier work of Lamb.<sup>7</sup> Although both papers deal with detuning and multimode operation, there are considerable differences in formulation and method of solution, so that direct comparison in some cases is impossible. In Lamb's work the analysis is not restricted to an optically pumped system, but the rate of excitation is an unknown parameter of the problem. The only source of line broadening is radiation damping and the validity of the results are restricted to low levels of lasing intensity. Finally, the role of atomic motion is incorporated in an *ad hoc* fashion since the velocity distribution is not part of the self-consistent solution of the problem. On the other hand, by retaining the phase of the electromagnetic field, and by introducing a quantum-mechanical treatment of the excited population, Lamb's treatment is capable of making rather refined predictions on a number of important phenomena, which are intrinsically unobtainable here (frequency pulling and mode locking, for example).

The situation which Lamb refers to as the Doppler limit is essentially the case in which the line broadening due to radiation damping is much less than the Doppler width. Most of Lamb's results apply to this situation, and the corresponding limit in the present work is  $b \ll 1$ .

In this limit for single-mode operation, both

approaches predict that the threshold for the onset of oscillation increases with cavity detuning in proportion to  $e^{\phi^2}$ . In addition, both find that the power output passes through a local minimum when the cavity is tuned to the center of the atomic resonance, and that this effect will disappear as  $b$  becomes larger.

For multimode operation, Lamb distinguishes between two possible situations: "weak coupling" and "strong coupling." For weak coupling two or more modes can coexist in stable oscillation, while for strong coupling there is a tendency for one mode to suppress the other. Weak coupling is favored in the Doppler limit. Again, a similar picture emerges from the present work. For  $b \ll 1$  and  $\phi_c \geq 8b$ , two or more modes usually interact with separate excited populations and will not interfere with each other. For  $\phi_c < 4b$ , some degree of mode competition will always occur, and there are situations in which one mode will suppress the other entirely. Thus the situation  $\phi_c \geq 8b$ ,  $b \ll 1$ , and nonoverlapping holes may be identified with the weak-coupling case, and  $\phi_c < 8b$  or  $b \gg 1$  with strong coupling.

In the present work, the neglect of the phase of the radiation means that frequency-pulling or frequency-locking phenomena cannot be treated. However, the frequency pulling could be found to a good approximation by first assuming that oscillation occurred at the cavity resonance. One would then evaluate the gain as has been done here, and use the Kramers-Krönig relations to calculate the phase shifts introduced by the active medium, as was done by Bennett.<sup>10</sup>

In conclusion, it seems that using kinetic equations and the equation of radiative transfer to describe the gas laser is conceptually and mathematically simpler than the semi-quantum-mechanical self-consistent field approaches and provides similar results within its domain of applicability. Further, the method is not restricted to low levels of lasing intensity and provides a clear description of effects due to line broadening and atomic motion, through the velocity distribution function. Ultimately, however, the kinetic approach may be most fruitful in applications in which a flow process is intrinsic to the lasing activity, as, for example, in gas dynamic and chemical lasers. The kinetic description seems particularly appropriate here, and this type of problem will be treated in a forthcoming paper.

#### ACKNOWLEDGMENTS

The authors wish to thank Professor H. J. Geritsen for several helpful discussions. This work was supported by the Mechanics Division, Office of Aerospace Research, under Contract-No. F44620-71-C-0030.

## APPENDIX: EVALUATION OF SYSTEM GAIN

We are interested in the behavior of the integral over  $n_x$  in Eq. (14) of the text. Thus, we have

$$I \equiv \int_{-\infty}^{\infty} \frac{d\eta_x H(b + \zeta_{21} - \eta_x) H(b - \zeta_{21} + \eta_x) e^{-\eta_x^2}}{[4\pi(A_{20} + A_{21}) + \sigma_2](4\pi A_{10} + \sigma_1) + A_{21} Q_{21}^{(0)} [4\pi(A_{20} + A_{10}) + \sigma_1 + \sigma_2]} , \quad (A1)$$

$$Q_{21}^{(0)} \equiv \frac{\pi L^0}{b} [H(b - |\phi| - \eta_x) H(b + |\phi| + \eta_x) + H(b - |\phi| + \eta_x) H(b + |\phi| - \eta_x)] .$$

As an example we will consider the case where  $|\phi| \leq b$  and  $0 \leq |\zeta_{21}| \leq |\phi|$ . The behavior of the various Heaviside functions in this particular case is shown in Fig. 15. Thus for  $0 \leq |\zeta_{21}| \leq |\phi| \leq b$ , we have

$$I = \int_{-(b-\zeta_{21})}^{-(b-\phi)} \frac{d\eta_x e^{-\eta_x^2}}{[4\pi(A_{20} + A_{21}) + \sigma_2](4\pi A_{10} + \sigma_1) + (\pi A_{21} L^0/b) [4\pi(A_{20} + A_{10}) + \sigma_1 + \sigma_2]} + \int_{-(b-\phi)}^{b-\phi} \frac{d\eta_x e^{-\eta_x^2}}{[4\pi(A_{20} + A_{21}) + \sigma_2](4\pi A_{10} + \sigma_1) + (2\pi A_{21} L^0/b) [4\pi(A_{20} + A_{10}) + \sigma_1 + \sigma_2]} + \int_{b-\phi}^{b+\zeta_{21}} \frac{d\eta_x e^{-\eta_x^2}}{[4\pi(A_{20} + A_{21}) + \sigma_2](4\pi A_{10} + \sigma_1) + (\pi A_{21} L^0/b) [4\pi(A_{20} + A_{10}) + \sigma_1 + \sigma_2]} = \frac{\sqrt{\pi}}{2[4\pi(A_{20} + A_{21}) + \sigma_2](4\pi A_{10} + \sigma_1)} \left( \frac{\operatorname{erf}(b + \zeta_{21}) + \operatorname{erf}(b - \zeta_{21}) - 2\operatorname{erf}(b - \phi)}{1 + x} + \frac{2\operatorname{erf}(b - \phi)}{1 + 2x} \right) , \quad (A2)$$

where

$$x \equiv \frac{\pi A_{21} L^0}{b} \frac{4\pi(A_{10} + A_{20}) + \sigma_1 + \sigma_2}{[4\pi(A_{20} + A_{21}) + \sigma_2](4\pi A_{10} + \sigma_1)} \quad \text{and} \quad \operatorname{erfb} \equiv \frac{2}{\sqrt{\pi}} \int_0^b e^{-y^2} dy .$$

For  $L^0 = 0$  and  $\zeta_{21} = 0$ , (A2) reduces to

$$I(L^0 = 0; \zeta_{21} = 0) = \frac{\sqrt{\pi} 2 \operatorname{erfb}}{2[4\pi(A_{20} + A_{21}) + \sigma_2](4\pi A_{10} + \sigma_1)} . \quad (A3)$$

From (A2), (A3), and the definition (16), we can then write

$$\tilde{G} = \frac{\operatorname{erf}(b + \zeta_{21}) + \operatorname{erf}(b - \zeta_{21}) - 2\operatorname{erf}(b - \phi)}{2 \operatorname{erfb} (1 + x)} + \frac{\operatorname{erf}(b - \phi)}{\operatorname{erfb} (1 + 2x)} , \quad 0 \leq \zeta_{21} \leq \phi \leq b$$

which is Eq. (17a) of the text. The evaluation for all other values of  $\zeta_{21}$ ,  $\phi$ , and  $b$  proceeds in a similar fashion.

For  $b \leq \phi \leq 2b$ , we find

$$\tilde{G} = \frac{\operatorname{erf}(b + \zeta_{21}) + \operatorname{erf}(b - \zeta_{21}) - 2\operatorname{erf}(\phi - b)}{2 \operatorname{erfb} (1 + x)} + \frac{\operatorname{erf}(\phi - b)}{\operatorname{erfb}} , \quad 0 \leq \zeta_{21} \leq 2b - \phi$$

$$\tilde{G} = \frac{\operatorname{erf}(b + \zeta_{21}) - \operatorname{erf}(\phi - b)}{2 \operatorname{erfb} (1 + x)} + \frac{\operatorname{erf}(\phi - b) + \operatorname{erf}(b - \zeta_{21})}{2 \operatorname{erfb}} , \quad 2b - \phi \leq \zeta_{21} \leq \phi$$

$$\tilde{G} = \frac{\operatorname{erf}(b + \phi) - \operatorname{erf}(\zeta_{21} - b)}{2 \operatorname{erfb} (1 + x)} + \frac{\operatorname{erf}(b + \zeta_{21}) - \operatorname{erf}(b + \phi)}{2 \operatorname{erfb}} , \quad \phi \leq \zeta_{21} \leq 2b + \phi$$

$$\tilde{G} = \frac{\operatorname{erf}(\zeta_{21} + b) - \operatorname{erf}(\zeta_{21} - b)}{2 \operatorname{erfb}} , \quad 2b + \phi \leq \zeta_{21} \leq \infty .$$

For  $\phi \geq 2b$ , we find

$$\tilde{G} = \frac{\operatorname{erf}(b + \zeta_{21}) - \operatorname{erf}(\zeta_{21} - b)}{2 \operatorname{erfb}} , \quad 0 \leq \zeta_{21} \leq \phi - 2b$$

$$\tilde{G} = \frac{\operatorname{erf}(\zeta_{21} + b) - \operatorname{erf}(\phi - b)}{2 \operatorname{erfb} (1 + x)} + \frac{\operatorname{erf}(\phi - b) - \operatorname{erf}(\zeta_{21} - b)}{2 \operatorname{erfb}} , \quad |2b - \phi| \leq \zeta_{21} \leq \phi$$

$$\tilde{G} = \frac{\operatorname{erf}(b + \phi) - \operatorname{erf}(\zeta_{21} - b)}{2 \operatorname{erfb} (1 + x)} + \frac{\operatorname{erf}(b + \zeta_{21}) - \operatorname{erf}(b + \phi)}{2 \operatorname{erfb}} , \quad \phi \leq \zeta_{21} \leq 2b + \phi$$

$$\tilde{G} = \frac{\operatorname{erf}(b + \zeta_{21}) - \operatorname{erf}(\zeta_{21} - b)}{2 \operatorname{erfb}} , \quad 2b + \phi \leq \zeta_{21} \leq \infty .$$

<sup>1</sup>J. W. Cipolla, Jr. and T. F. Morse, *Phys. Fluids* **14**, 1850 (1971).

<sup>2</sup>L. M. Biberman, *Zh. Eksperim. i Teor. Fiz.* **19**, 584 (1949).

<sup>3</sup>T. Holstein, *Phys. Rev.* **72**, 1212 (1947); **83**, 1159 (1951).

<sup>4</sup>(a) J. J. Healy and T. F. Morse, *J. Quant. Spectry. Radiative Transfer* (to be published); (b) J. J. Healy, Ph. D. thesis (Brown University, 1972) (unpublished).

<sup>5</sup>R. J. Gelinis, *Phys. Rev.* **175**, 300 (1968).

<sup>6</sup>R. J. Gelinis and R. L. Ott, *Ann. Phys. (N. Y.)* **59**, 323 (1970).

<sup>7</sup>W. E. Lamb, Jr., *Phys. Rev.* **184**, A1429 (1964).

<sup>8</sup>(a) S. Jacobs, G. Gould, and P. Rabinowitz, *Phys.*

*Rev. Letters* **11**, 415 (1961). (b) P. Rabinowitz, S. Jacobs, and G. Gould, *Appl. Opt.* **1**, 513 (1962). (c) P. Rabinowitz and S. Jacobs, in *Quantum Electronics*, edited by P. Grivet and N. Blombergen (Columbia U. P., New York, 1964), p. 489.

<sup>9</sup>W. Christiansen (private communication).

<sup>10</sup>W. R. Bennett, Jr., in *Lasers, A Collection of Reprints with Commentary*, edited by J. Weber (Gordon and Breach, New York, 1968), Vol. 10A.

<sup>11</sup>B. A. Lengyel, *Lasers* (Wiley, New York, 1971), pp. 282-285.

<sup>12</sup>A. Szoke and A. Javan, *Phys. Rev. Letters* **10**, 521 (1963).

PHYSICAL REVIEW A

VOLUME 6, NUMBER 6

DECEMBER 1972

## Low-Temperature Expansion of the Third-Cluster Coefficient of a Quantum Gas

W. G. Gibson

*Department of Applied Mathematics, The University of Sydney, N. S. W. 2006, Australia*

(Received 1 June 1972)

The low-temperature behavior of the third-quantum-cluster coefficient is investigated using the multiple-scattering form of the binary-collision expansion. For hard spheres and Boltzmann statistics we find

$$b_3 = 2(a/\lambda)^2 - \frac{4}{3}\sqrt{2}\pi(a/\lambda)^3 - \frac{16}{3}(4\pi - 3\sqrt{3})(a/\lambda)^4 \ln(a/\lambda) + O((a/\lambda)^4),$$

where  $a$  is the sphere diameter and  $\lambda$  is the thermal wavelength. The first two terms were obtained some time ago by Lee and Yang and by Pais and Uhlenbeck. The occurrence of a term of the form  $\lambda^{-4} \ln \lambda$  was predicted recently by Adhikari and Amado. The expansion is also given for Bose-Einstein and Fermi-Dirac statistics, and for the case of an intermolecular potential without bound states. The limitations of such low-temperature expansions are discussed.

### I. INTRODUCTION

For a classical gas, the cluster coefficients  $b_l$  (and hence the virial coefficients) can be expressed as integrals over functions of the two-body potential. Thus their evaluation involves a series of quadratures.

In the quantum case, the connection between the cluster coefficients and the intermolecular potential is not nearly so direct. Only for the second coefficient  $b_2$  is there available an exact expression<sup>1</sup> which allows its computation over a wide temperature range. There exist formal expressions for the third<sup>2-4</sup> and higher<sup>5-8</sup> coefficients, but these have not as yet been used for any extensive calculations.

The limiting case of low temperatures has been studied using the binary-collision expansion<sup>9</sup> and the related pseudopotential method.<sup>10</sup> For the hard-sphere gas Lee and Yang<sup>11</sup> evaluated  $b_l$  as a series in powers of  $a/\lambda$  as far as the term in  $(a/\lambda)^2$ . [ $a$  is the sphere diameter and  $\lambda = (2\pi\hbar^2/mkT)^{1/2}$  is the thermal wavelength.] Pais and Uhlenbeck<sup>12</sup> extended this to the term in  $(a/\lambda)^3$  for  $b_3$ . From this

it might appear that we have the leading terms of an expansion for  $b_l$  in powers of  $(a/\lambda)$ .<sup>13</sup> However, Adhikari and Amado<sup>14</sup> have recently shown that the low-temperature expansions of cluster coefficients higher than the second<sup>15</sup> involve  $\ln \lambda$  as well as powers of  $\lambda$ . In particular, the third-cluster coefficient (for Boltzmann statistics) has the expansion

$$b_3 = c_1/\lambda^2 + c_2/\lambda^3 + c_3(\ln \lambda)/\lambda^4 + O(\lambda^{-4}), \quad (1)$$

where the  $c_i$  depend only on the hard-sphere diameter, or more generally on the two-body  $s$ -wave scattering length. The coefficient  $c_3$  can be found from the leading terms of the binary-collision expansion, and we shall present its explicit calculation below. However this is as far as we can go by present methods. The evaluation of the coefficient of the  $\lambda^{-4}$  term involves a solution of the full three-body problem, and this is a calculation of a higher order of difficulty.

It should be mentioned that other quantities relating to many-particle systems have logarithmic terms in their expansions. In particular, the low-density expansion of the ground-state energy of a system of bosons<sup>16</sup> or of fermions<sup>17,18</sup> contains a